

UC Davis

UC Davis Previously Published Works

Title

Integration of Silver Nanoparticle-impregnated Polyelectrolyte Multilayers Into Murine-Splinted Cutaneous Wound Beds

Permalink

<https://escholarship.org/uc/item/1rv9b71m>

Journal

Journal of Burn Care & Research, 34(6)

ISSN

1559-047X

Authors

Guthrie, Kathleen M
Agarwal, Ankit
Teixeira, Leandro BC
[et al.](#)

Publication Date

2013

DOI

10.1097/bcr.0b013e31827e7ef9

Peer reviewed



Published in final edited form as:

J Burn Care Res. 2013 ; 34(6): e359–e367. doi:10.1097/BCR.0b013e31827e7ef9.

Integration of silver nanoparticle-impregnated polyelectrolyte multilayers into murine splinted cutaneous wound beds

Kathleen M. Guthrie, DVM¹, Ankit Agarwal, PhD², Leandro B. C. Teixeira, MS, DVM³, Richard R. Dubielzig, DVM³, Nicholas L. Abbott, PhD², Christopher J. Murphy, DVM, PhD^{1,4,5}, Harpreet Singh, BS, DVM⁷, Jonathan F. McAnulty, DVM, PhD¹, and Michael J. Schurr, MD⁶

¹University of Wisconsin, School of Veterinary Medicine, Department of Surgical Sciences

²University of Wisconsin, Department of Chemical and Biological Engineering

³University of Wisconsin, School of Veterinary Medicine, Department of Pathobiological Sciences

⁴UC Davis, School of Medicine, Department of Ophthalmology and Vision Science

⁵UC Davis, School of Veterinary Medicine, Department of Surgical and Radiological Sciences

⁶University of Colorado-Denver, School of Medicine, Department of Surgery

⁷Tufts University, Cummings School of Veterinary Medicine

Abstract

Silver is a commonly used topical antimicrobial. However, technologies to immobilize silver at the wound surface are lacking, while currently available silver-containing wound dressings release excess silver that can be cytotoxic and impair wound healing. We have shown that precise concentrations of silver at lower levels can be immobilized into a wound bed using a polyelectrolyte multilayer (PEM) attachment technology. These silver nanoparticle-impregnated PEMs are non-cytotoxic yet bactericidal *in vitro*, but their effect on wound healing *in vivo* was previously unknown.

Objective—The purpose of this study was to determine the effect on wound healing of integrating silver nanoparticle/PEMs into the wound bed.

Methods—A full-thickness, splinted, excisional murine wound healing model was employed in both phenotypically normal mice and spontaneously diabetic mice (healing impaired model).

Results—Gross image measurements showed an initial small lag in healing in the silver-treated wounds in diabetic mice, but no difference in time to complete wound closure in either normal or

Corresponding author: Jonathan F. McAnulty, DVM, Ph.D., (Also use for reprint requests), University of Wisconsin, School of Veterinary Medicine, Department of Surgical Sciences, 2015 Linden Drive, Madison, WI 53706, Phone: 608-265-2455, Fax: 608-263-7930, mcanultj@svm.vetmed.wisc.edu.

Publisher's Disclaimer: This is a PDF file of an unedited manuscript that has been accepted for publication. As a service to our customers we are providing this early version of the manuscript. The manuscript will undergo copyediting, typesetting, and review of the resulting proof before it is published in its final citable form. Please note that during the production process errors may be discovered which could affect the content, and all legal disclaimers that apply to the journal pertain.

Conflicts of interest: Authors Agarwal, Abbott, Murphy, Schurr, and McAnulty are founding members of Imbed Biosciences, Inc.

diabetic mice. Histological analysis showed modest differences between silver-treated and control groups on day 9, but no difference between groups at the time of wound closure.

Conclusions—We conclude that silver nanoparticle/PEMs can be safely integrated into the wound beds of both normal and diabetic mice without delaying wound closure, and with transient histological effects. The results of this study suggest the feasibility of this technology for use as a platform to effect nanoscale wound engineering approaches to microbial prophylaxis or to augment wound healing.

Keywords

silver nanoparticles; murine; wound; polyelectrolyte multilayers; splinted

Introduction

Silver has been used for many years to prevent and treat wound infections. Silver is advantageous because of its broad spectrum of activity¹, including efficacy against fungi² and antibiotic-resistant bacteria.^{3,4} There are many commercial wound dressings available that contain silver⁵, but recent research has shown that the concentrations of silver released from these dressings are cytotoxic^{6–8}, may impair wound healing⁹, and may even cause systemic illness.^{10,11} The ability to integrate a concentration of silver directly into wound beds that is non-cytotoxic to host tissue and still exhibits antibacterial efficacy would be a significant advancement in the treatment of burn wounds.

The use of nanoparticulate silver in nanometer-thick polyelectrolyte multilayer (PEM) films was recently described.¹² These films are comprised of alternating layers of oppositely charged polyelectrolytes poly(allylamine hydrochloride) (PAH) and poly(acrylic acid) (PAA). The PEMs are assembled through a layer-by-layer deposition process, and precise loadings of silver nanoparticles can be impregnated within the films.¹² As shown by *in vitro* studies, silver at concentrations of $\sim 0.4 \mu\text{g}/\text{cm}^2$ or less in PEMs exhibited no cytotoxic effects to mammalian fibroblasts, but were bactericidal against *Staphylococcus epidermidis*.¹² Further work with silver nanoparticle-impregnated PEMs (silver NP/PEMs) demonstrated that they can be integrated onto the dermal surface of a skin substitute, gamma-irradiated human cadaver skin (GammaGraft[®], Promethean LifeSciences, Inc.), and exert bactericidal activity against *S. epidermidis* and *Pseudomonas aeruginosa* ATCC[®] 27853TM.¹³ Subsequent data from our laboratory confirmed that silver NP/PEMs exhibited bactericidal activity against *Staphylococcus aureus* subsp. *aureus* ATCC[®] 25923TM *in vivo*.¹⁴

Although the *in vitro* studies showed that silver NP/PEMs were not cytotoxic to murine fibroblasts, the *in vivo* effect on wound healing remained unknown. The purpose of this study was to determine whether the presence of silver NP/PEMs in a wound bed would be a detriment to wound healing. A full-thickness, excisional, splinted wound model in mice was employed. The splinted wound model has been shown to decrease wound contraction in mice, allowing epithelialization to play a more prominent role in healing and more closely mimic human wound healing.¹⁵ The studies were performed in both phenotypically normal and genetically diabetic mice, as models of normal and impaired¹⁶ wound healing, respectively. We hypothesized that the application and presence of silver NP/PEMs within

the wound bed would not impair wound healing in the diabetic mice or their heterozygous (phenotypically normal) littermates. We also hypothesized that diabetic mice would have impaired wound healing in this excisional splinted model, compared to heterozygous mice.

Methods

Silver nanoparticle-impregnated PEMs

Materials and methods used to fabricate PEMs were adapted from a previous study.¹³ Briefly, PEMs of oppositely charged weak polyelectrolytes poly(allylaminehydrochloride) (PAH) (Mw=70 kDa; Sigma Aldrich, St. Louis, MO) and poly(acrylic acid) (PAA) (Mw=60 kDa; Polysciences, Warrington, PA) were assembled on elastomeric poly(dimethylsiloxane) (PDMS) sheets by alternate 'layer-by-layer' deposition using a StratoSequence Robot (nanoStrata Inc, Tallahassee, FL). The PDMS sheets were sequentially incubated in solutions of PAA (pH 5.5) and PAH (pH 7.5), at 0.01 M by repeat unit, for 10 minutes each, and rinsed with Milli-Q™ (Millipore Corporation) water three times after immersion in polyelectrolyte solutions. Following deposition of 10 bilayers of PAH and PAA, a monolayer of negatively charged carboxylate-modified polystyrene microspheres (crimson fluorescent, Ext/Em- 625/645 nm; Invitrogen, Carlsbad, CA) was assembled, as described elsewhere.¹³ Additional bilayers of PAH and strong polyelectrolyte poly(styrenesulfonate) (PSS; Mw=70 kDa, Sigma) were assembled over the microspheres to facilitate deposition of poly(vinylpyrrolidone) (PVP)-coated silver nanoparticles (20 nm diameter) obtained from NanoAmor, Inc (Houston, TX).¹⁷⁻¹⁹ A 0.2 wt% suspension of silver nanoparticles in water, adjusted to pH 2.0 using nitric acid to protonate PVP, was incubated for 30 minutes over PEMs ending in negatively charged PSS, and subsequently rinsed with water. The silver nanoparticle layer was finally capped with bilayers of PAH and PAA. The final structure of the PEMs used in this study can be denoted as PAH(PAA/PAH)₁₀(PS-microspheres)(PAH/PSS)₂(AgNP)(PAA/PAH)₂. Silver loading in PEMs was determined by extracting silver from the films in 2% nitric acid over 24 hours and measuring extracted silver-ion concentrations using inductively-coupled plasma emission spectroscopy (ICP-ES) as described elsewhere.¹² Sustained cumulative release of silver from the PEMs in Milli-Q™ water was measured every 24 hours for 10 days.

A pilot study was conducted to evaluate the ability to transfer the PEMs into the wound beds. Fluorescently labeled microspheres were incorporated within the PEMs, and the PEMs, supported by the PDMS sheets, were mechanically transferred to the wound beds by applying approximately 200 kPa of pressure. The transfer of PEMs was confirmed visually by identifying the fluorescence within the wound bed. Silver extraction was performed on the PDMS sheets following transfer, to quantify the amount of silver that remained.

For the present study, PDMS sheets supporting silver-nanoparticle/PEMs were cut to the size of the wounds and the PEMs were mechanically transferred onto the wound beds. This was established with an approximate pressure of 200 kPa applied on PDMS sheets against the wounds until transfer of the PEMs was confirmed visually. Although the microspheres of the PEMs were not fluorescently labeled for the *in vivo* portion of this study, transfer of the PEMs, as indicated by transfer of the color associated with the silver nanoparticles, could be visualized with the naked eye.

Mice

Genetically diabetic (*db/db*) male mice and their phenotypically normal heterozygous littermates (*Lepr^{db}*, Jackson Laboratories, Inc.) between the ages of 8–12 weeks were used for the studies. Mice were housed in groups during a one-week acclimation period prior to the study and housed individually post-operatively. Mice were maintained in a temperature-controlled facility with a standard light/dark cycle and were provided with environmental enrichment, and food and water *ad libitum*.

Procedures

All experimental protocols were approved by the Institutional Animal Care and Use Committee (IACUC) of the relevant institution. Mice were anesthetized in an induction chamber with inhaled isoflurane. The hindlimb nails were clipped to prevent trauma to the wounds. The mice were injected subcutaneously with buprenorphine (0.1 mg/kg) for pain control and the cranial thoracodorsal region was shaved and aseptically prepared for surgery. Two silicone O-rings (McMaster-Carr®, inner diameter 11 mm, outer diameter 15 mm) were applied to the skin four mm caudal to the base of the ears, one on either side of the dorsal midline, and secured with cyanoacrylic tissue glue (Instant Krazy Glue® Gel; Elmer's Products, Inc.) and eight 5-0 interrupted nylon sutures. The O-rings served as splints and were used to decrease contraction of the wound margins over the course of the study.¹⁵ Sterile 6-mm biopsy punches were used to create two symmetrical wounds centered in the skin surrounded by the two O-rings in each mouse. Wounds were left uncovered and the mice were recovered from anesthesia on a warming pad. Mice were monitored daily for signs of pain and illness. Mice were weighed on days 0, 1, and 3 post-operatively, and every three days thereafter. At the end of the study, mice were euthanatized by injection of Beuthanasia®-D (Schering-Plough) solution (0.5 ml/mouse) intraperitoneally after induction of anesthesia as described above.

Mice were randomly assigned to either the control or experimental groups on the day of surgery (10 *db/db* or heterozygous mice per group, total n = 40 mice). Control mice received no treatment. Silver NP/PEMs were transferred to the wounds of the mice in the experimental group as described above.

For the duration of the studies, the splints and sutures were monitored daily. Any loss of contact between the splint and skin was repaired with cyanoacrylate tissue glue. Broken or missing sutures were replaced under anesthesia as described above, and buprenorphine was administered subcutaneously (0.1 mg/kg) for pain control. Wounds were censored from analysis if two or more sutures were broken or missing within a 24-hour period.

Wound analysis

Wounds were photographed on days 0, 1, and 3 post-operatively, and every two to three days thereafter. Wound edges were traced in the digital images and the area calculated using ImageJ²⁰ software. Wound closure was reported at each time point as the remaining percentage of the original wound area. On post-operative day 9, five mice in each group were euthanatized and the wounds were harvested for histological analysis. The remaining

mice were followed until complete wound closure and euthanatized at that time. Healed wounds were also harvested for histological analysis.

For histopathology, harvested tissue was fixed in 10% buffered formalin for at least 24 hours, and subsequently sectioned through the center of the lesion. After routine paraffin processing, tissue samples were serially sectioned at a thickness of 5 μm , making sure to include the center of the lesion on the slide. Slides were stained with hematoxylin and eosin and by picosirius red. A mounted digital camera (Olympus DP72, Melville, NY) was used to photograph the sections using light microscopy. Four parameters were evaluated on each slide containing the center of the lesion: length of re-epithelialization, length of the epithelial gap, amount of fibrovascular proliferation in the dermis, and inflammatory response scores. Measurements were taken and analyzed using software (CellSence Dimension 1.4, Olympus, Melville, NY). Length of re-epithelialization was defined by the length of the layer of proliferating keratinocytes in the wound bed, and was calculated by measuring the distance between the free edge of the keratinocyte layer and the base where the cells were still associated with native dermal tissue (Figure 1). The measurements from each side of the wound were added together for one value. For wounds that were completely re-epithelialized, a single measurement was taken from base to base. The epithelial gap was defined as the area of the wound not covered by advancing keratinocytes (Figure 1A and B). Inflammation was subjectively assessed by evaluating infiltrates of lymphocytes, plasma cells, macrophages and neutrophils using a semi-quantitative scoring system ranging from 0 to 4 where 0 indicates no inflammation, 1 indicates 0–25% of the wound area affected, 2 indicates 25–50% of the wound area affected, 3 indicates 50–75% of the wound area affected, and 4 indicates >75% of the wound area affected (Figure 2A, B and C). Fibrovascular dermal proliferation was measured by calculating the relative amount of collagen in the wound bed compared to other types of tissue, highlighted by picosirius red stain under polarized light (Figure 3A, B and C). Image analysis software ImageJ was used to measure the percentage of the wound area composed of collagen. A single author (LT) analyzed the histological data, and this author was blinded to the treatment group of each sample.

Statistical analysis

Statistical analysis was performed using SigmaPlot[®] software (Systat Software, Inc.). Each wound was analyzed individually. All normally distributed data were analyzed by Student's t-test. All non-normally distributed data were analyzed by Mann-Whitney U test. Significance was set at $p < 0.05$. Values stated are mean \pm standard error of the mean (SEM).

Results

All mice completed the study with no mortality, surgical complications, signs of pain, illness, or significant weight loss, as defined by a loss of >10% body weight. Four heterozygous wounds (3 control and 1 silver-treated) and five *db/db* wounds (all silver-treated, including both wounds of two mice) were excluded from the study because of loss of multiple sutures. Silver loading into the PEMs, as measured by plasma emission

spectroscopy was $11.58 \pm 2.33 \mu\text{g}/\text{cm}^2$. Daily silver release from the PEMs into Milli-Q™ water measured approximately $1 \mu\text{g}/\text{cm}^2$ (Figure S1). The concentration of silver remaining on PDMS sheets after transfer of the PEMs onto the wound surface was $1.63 \pm 0.49 \mu\text{g}/\text{cm}^2$, meaning greater than 85% of silver was successfully transferred from PDMS sheets onto the wound bed.

All heterozygous mice that were followed to wound closure had bilaterally healed wounds by day 18 post-operatively. Control wounds healed between post-operative days 11 through 18 (15.8 ± 0.4 days), and silver-treated wounds healed between post-operative days 14 through 18 (16.2 ± 0.3 days). The wound appearances were grossly similar between both groups throughout all time points (Figure 4). On day 3, the silver-treated group had a modest but statistically significant increased wound closure compared to the control group ($p < 0.001$), although there were no differences noted at any other time point (Figure 5).

All *db/db* mice followed to wound closure had bilaterally healed wounds by day 22 post-operatively. Control diabetic wounds healed between post-operative days 12 through 22 (17.7 ± 1 days), and silver-treated wounds healed between post-operative days 18 through 22 (20.7 ± 0.8 days). Wound closure of silver-treated wounds was significantly less on days 3 ($p=0.041$), 6 ($p=0.001$), and 9 ($p=0.017$) but this difference was lost by day 12 and thereafter (Figure 6).

Histological analysis of wounds harvested on post-operative day 9 showed that heterozygous mice in both groups had comparable wound sizes and length of re-epithelialization measurements (Table 1). The silver NP/PEM group exhibited a higher percentage of collagen, approximately a 9% increase over controls, within the wound ($p=0.01$). There were no significant differences in the studied histologic parameters at the end of the study.

Significant differences indicative of an initial delay in wound healing were present for all histologic parameters measured in the diabetic groups on day 9 (Table 2). Wounds in the silver NP/PEM group were larger with a greater epithelial gap ($p<0.001$), had less re-epithelialization ($p=0.008$), exhibited a higher inflammation score ($p=0.011$), and had a lower percentage of collagen in the wound ($p=0.011$) at that time point. However, histopathological analysis of diabetic wounds at the end of the study showed no significant differences between groups when evaluating re-epithelialization, epithelial gap, percentage of collagen, and inflammation score.

Discussion

In this report, we show that silver NP/PEMs can be successfully incorporated into the wound beds of mice without delaying complete wound closure. These studies highlight a fundamentally different approach to wound management that allows incorporation of low concentrations of silver directly into the wound bed by a facile method of transfer. The low concentrations of silver released from the PEMs are up to 100 times less than the amount of silver released in commonly used current commercial dressings, which serve as a macroscopic reservoir from which silver must diffuse through wound fluid.¹³ The integration of the silver NP/PEMs into the wound bed represents a novel approach, as this

allows for active incorporation of silver-loaded PEMs into the wound surface and direct bioengineering of the wound bed. The advantage of this approach is that silver is delivered and immobilized directly at the site of action, bypassing the necessity for diffusion through the wound fluid where the majority of silver would be deactivated by protein binding.⁵ This allows increased effectiveness of the antimicrobial agent at the site of action and use of lower concentrations of silver while retaining antimicrobial efficacy. These low, yet antibacterial, concentrations of silver used in the PEMs have previously been shown to be non-cytotoxic *in vitro*.¹²

It must be recognized that *in vitro* assays examining specific concentrations of silver for cytotoxic and antibacterial effects may not directly relate to the *in vivo* situation but provide proof of principle that a therapeutic window exists where antibacterial efficacy can be achieved without significant cell toxicity. *In vivo*, some degree of silver ion inactivation would be expected through reaction with nearby proteins. Thus, it is anticipated that the effective therapeutic concentration window *in vivo* for this approach would be frame-shifted upward somewhat compared to previous *in vitro* studies. In this study, we found that the constructed silver NP/PEMs released approximately 1 $\mu\text{g}/\text{cm}^2$ into water and that 85% of the silver on the PDMS template transferred to the wound, resulting in an estimated release of approximately 0.85 $\mu\text{g}/\text{cm}^2$ silver in the wound bed. This concentration of silver, although slightly higher than that previously shown to be non-cytotoxic in *in vitro* assays, did not impair wound closure in this study, validating earlier conclusions that the use of PEMs for immobilization of silver at the wound surface represents a nontoxic technology for wound surface modification and antimicrobial prophylaxis.

In heterozygous mice, the histological analysis corroborated image analysis results, with no significant differences between the groups regarding epithelial gap and re-epithelialization, relative to wound size. The silver-treated group exhibited a significantly greater percentage of collagen in the wounds than the control group on post-operative day 9. Although not statistically significant, there was also a trend for the silver-treated group to exhibit a higher inflammation score compared to the control group. One potential cause for such a trend may relate to the experimental design of this study. In the current method for application of the PEMs to the wound bed, manual pressure of the PDMS template against the wound is required in order to successfully transfer the silver NP/PEMs from the PDMS to the wound bed. Pressure could cause some minor tissue damage, leading to the release of inflammatory mediators and an increase in the observed inflammatory reaction. An unpublished pilot study conducted in our laboratory evaluating the effect on wounds of stamping alone did not show a significant impact on wound closure in diabetic or heterozygous mice. That pilot study, however, was conducted in an unsplinted wound model; a model that is more dependent on wound contracture and less sensitive to low level tissue trauma. Although not included in the current study, a sham wound treatment control group would assist in clarifying the impact of tissue manipulation in the treated mice. Regardless, the wounds healed to closure in the same time period and the histological differences between groups seen on day 9 were not seen once the wounds were healed, indicating that any inflammatory effect related to either the wound manipulation or the silver NP/PEMs on the tissue was both minimal and transient.

In *db/db* mice, initial wound closure in the silver-treated group was slightly delayed compared to control mice early in the study as seen on days 3, 6, and 9, but this difference disappeared by days 12, 17, and 21. This early effect on healing may also relate to wound trauma due to pressure applied during affixation of the silver NP/PEMs. This was a particular concern in diabetic mice because of the pronounced layer of fat below the skin due to morbid obesity in the *db/db* strain of mouse. It is likely that these diabetic mice would be more susceptible to trauma due to excess fat in the wound base as well as from the systemic effects of diabetes. Despite this initial lag in wound healing, however, the silver-treated wounds closed at approximately the same time as the control wounds, and the histopathology on the wounds at the time of closure showed no differences between the two groups. These results indicate that even if the process of stamping or the presence of the silver NP/PEM within the wound bed had any negative effect on healing, the effect was short-lived and did not delay definitive wound closure.

Four heterozygous and five *db/db* wounds were not included in the statistical analysis because they each had more than one suture lost within a 24-hour period. The presence of the splint on the wound resists the contracting action of the panniculus carnosus muscle. As the wound attempts to contract, tension builds between the skin and the splint. Eventually one or more sutures may break, become untied, or be damaged by the mouse as the tension becomes too great. We have found that in our studies using the splinted model, all mice experience the loss of at least one suture during the course of the experiment. However, although some contraction occurs when a suture is broken, a pilot experiment prior to this study found that this effect was minimal and a consistent rate of wound closure achievable by repair of the suture and splint. The loss of two or more sutures in one day, an uncommon occurrence resulting in more contraction of the wound, was established as a criterion for exclusion of those wounds from both gross image and histological analysis to maintain homogeneity amongst the study animals. As hypothesized, splinted wounds in *db/db* mice did heal more slowly than in their heterozygous littermates. This was consistent with previous reports in the literature where impaired wound healing has been well documented in *db/db* mice with both unsplinted²¹⁻²³ and splinted¹⁵ full-thickness excisional wound models. Because the splinted wound model forces wounds to heal primarily by epithelialization, it is reasonable to conclude that *db/db* mice suffer from impaired epithelialization of their wounds, in addition to impaired contraction.

This study has some inherent limitations that should be considered in interpreting the results. A larger sample size is always desired, and may have enabled us to find small but significant differences between treatment groups. Additionally, the use of a rodent model makes it difficult to extrapolate the results directly to the human population although the use of a splinted wound model biases wound healing toward epithelialization and away from contracture, thus more relevant to human wound healing. Furthermore, wounds were not covered for ease of photography and to eliminate wound manipulations during the study period; this does not mimic the typical clinical picture where a dressing is usually placed over a wound. And finally, this study has focused on evaluation of silver NP PEMs in an excisional wound model and thus may not mirror a clinical setting where this technology may be used on partial-thickness wounds or more complex wound problems such as burns.

However, this initial study using an excisional wound model provides proof-of-principle that the engineering of a wound surface using a PEM-based technology is nontoxic and that further studies should be undertaken in different wound types, such as in a burn wound model and in large animal models such as swine where the skin is more similar to human skin.

In conclusion, we have determined that the integration of silver NP/PEMs onto the wound beds of *db/db* mice and their heterozygous littermates does not impair wound closure. Nanoscale engineering of the wound surface using PEMs as an immobilization strategy for cytoactive agents represents a novel approach to enhance the effectiveness of these agents and enable wound healing strategies encompassing control of spatial, temporal and concentration dependent characteristics of these agents at the wound surface. For control of microbial bioburden, silver NP/PEMs represent a new technology that holds promise for the treatment of chronic and burn wounds colonized or infected with bacteria. This study forms the basis for subsequent animal trials investigating the efficacy of these silver-NP/PEMs in wound infection models and is a logical step towards the regulatory approval of this technology for human clinical trials.

Supplementary Material

Refer to Web version on PubMed Central for supplementary material.

Acknowledgements

The authors would like to thank Tyler B. Nelson, BS, for his assistance with materials preparation; Patricia R. Kierski, Zachary N. Joseph, BS, Ann E. Heffernan, BS, Katharine R. Kierski, and Allison R. Clarke, BA, for their assistance with the research. The authors also wish to acknowledge the National Institutes of Health for providing funding for the research through an RC-2 grant.

Author Agarwal acknowledges support from a fellowship from the Ewing Marion Kauffman Foundation. The studies described here were funded in their entirety by an RC-2 grant from the National Institutes of Health.

References

1. Ip M, Lui SL, Poon VKM, et al. Antimicrobial activities of silver dressings: an in vitro comparison. *J Med Microbiol.* 2006; 55:59–63. [PubMed: 16388031]
2. Wright JB, Lam K, Hansen D, et al. Efficacy of topical silver against fungal burn wound pathogens. *Am J Infect Control.* 1999; 27:344–350. [PubMed: 10433674]
3. Wright JB, Lam K, Burrell RE. Wound management in an era of increasing bacterial antibiotic resistance: A role for topical silver treatment. *Am J Infect Control.* 1998; 26:572–577. [PubMed: 9836841]
4. Maple PAC, Hamilton-Miller JMT, Brumfitt W. Comparison of the in-vitro activities of the topical antimicrobials azelaic acid, nitrofurazone, silver sulphadiazine and mupirocin against methicillin-resistant *Staphylococcus aureus*. *J Antimicrob Chemother.* 1992; 29:661–668. [PubMed: 1506349]
5. Mooney EK, Lippitt C, Friedman J. Silver Dressings. *Plast Reconstr Surg.* 2006; 117:666–669. [PubMed: 16462356]
6. Lee AR, Moon HK. Effect of topically applied silver sulfadiazine on fibroblast cell proliferation and biomechanical properties of the wound. *Arch Pharmacol Res.* 2003; 26:855–860.
7. Van Den Plas D, De Smet K, Lens D, et al. Differential cell death programmes induced by silver dressings in vitro. *Eur J Dermatol.* 2008; 18:416–421. [PubMed: 18573715]

8. Poon VKM, Burd A. In vitro cytotoxicity of silver: implication for clinical wound care. *Burns*. 2004; 30:140–147. [PubMed: 15019121]
9. Innes ME, Umraw N, Fish JS, et al. The use of silver coated dressings on donor site wounds: a prospective, controlled matched pair study. *Burns*. 2001; 27:621–627. [PubMed: 11525858]
10. Trop M, Novak M, Rodl S, et al. Silver-coated dressing acticoat caused raised liver enzymes and argyria-like symptoms in burn patient. *J Trauma*. 2006; 60:648–652. [PubMed: 16531870]
11. Bador K. Organ deposition of silver following silver nitrate therapy for burns. *PRS*. 1966; 37:550.
12. Agarwal A, Weis TL, Schurr MJ, et al. Surfaces modified with nanometer-thick silver-impregnated polymeric films that kill bacteria but support growth of mammalian cells. *Biomaterials*. 2010; 31:680–690. [PubMed: 19864019]
13. Agarwal A, Guthrie KM, Czuprynski CJ, et al. Polymeric Multilayers that Contain Silver Nanoparticles can be Stamped onto Biological Tissues to Provide Antibacterial Activity. *Adv Funct Mater*. 2011; 21:1863–1873. [PubMed: 25558188]
14. Guthrie KM, Agarwal A, Tackes DS, et al. Antibacterial efficacy of silver-impregnated polyelectrolyte multilayers immobilized on a biological dressing in a murine wound infection model. *Ann Surg*. 2012; 256(2):371–377. [PubMed: 22609841]
15. Galiano R, Michaels V. Quantitative and reproducible murine model of excisional wound healing. *Wound Repair Regen*. 2004; 12:485–492. [PubMed: 15260814]
16. Greenhalgh D. Models of wound healing. *Journal of Burn Care & Research*. 2005; 26:293.
17. Podsiadlo P, Paternel S, Rouillard JM, et al. Layer-by-Layer Assembly of Nacre-like Nanostructured Composites with Antimicrobial Properties. *Langmuir*. 2005; 21:11915–11921. [PubMed: 16316133]
18. Sambhy V, MacBride MM, Peterson BR, et al. Silver Bromide Nanoparticle/Polymer Composites: Dual Action Tunable Antimicrobial Materials. *J Am Chem Soc*. 2006; 128:9798–9808. [PubMed: 16866536]
19. Yu DG, Lin WC, Yang MC. Surface Modification of Poly(L-lactic acid) Membrane via Layer-by-Layer Assembly of Silver Nanoparticle-Embedded Polyelectrolyte Multilayer. *Bioconjugate Chem*. 2007; 18:1521–1549.
20. ImageJ, U. S. National Institutes of Health. 1997–2011. Accessed at <http://imagej.nih.gov/ij/>.
21. Michaels J, Churgin S, Blechman K, et al. db/db mice exhibit severe wound healing impairments compared with other murine diabetic strains in a silicone splinted excisional wound model. *Wound Repair Regen*. 2007; 15:665–670. [PubMed: 17971012]
22. Iveti Tkal evi V, Cuzic S, Parnham M, et al. Differential Evaluation of Excisional Non-occluded Wound Healing in db/db Mice. *Toxicol Pathol*. 2009
23. Sullivan S, Underwood R, Gibran N, et al. Validation of a model for the study of multiple wounds in the diabetic mouse (db/db). *Plast Reconstr Surg*. 2004; 113:953. [PubMed: 15108888]

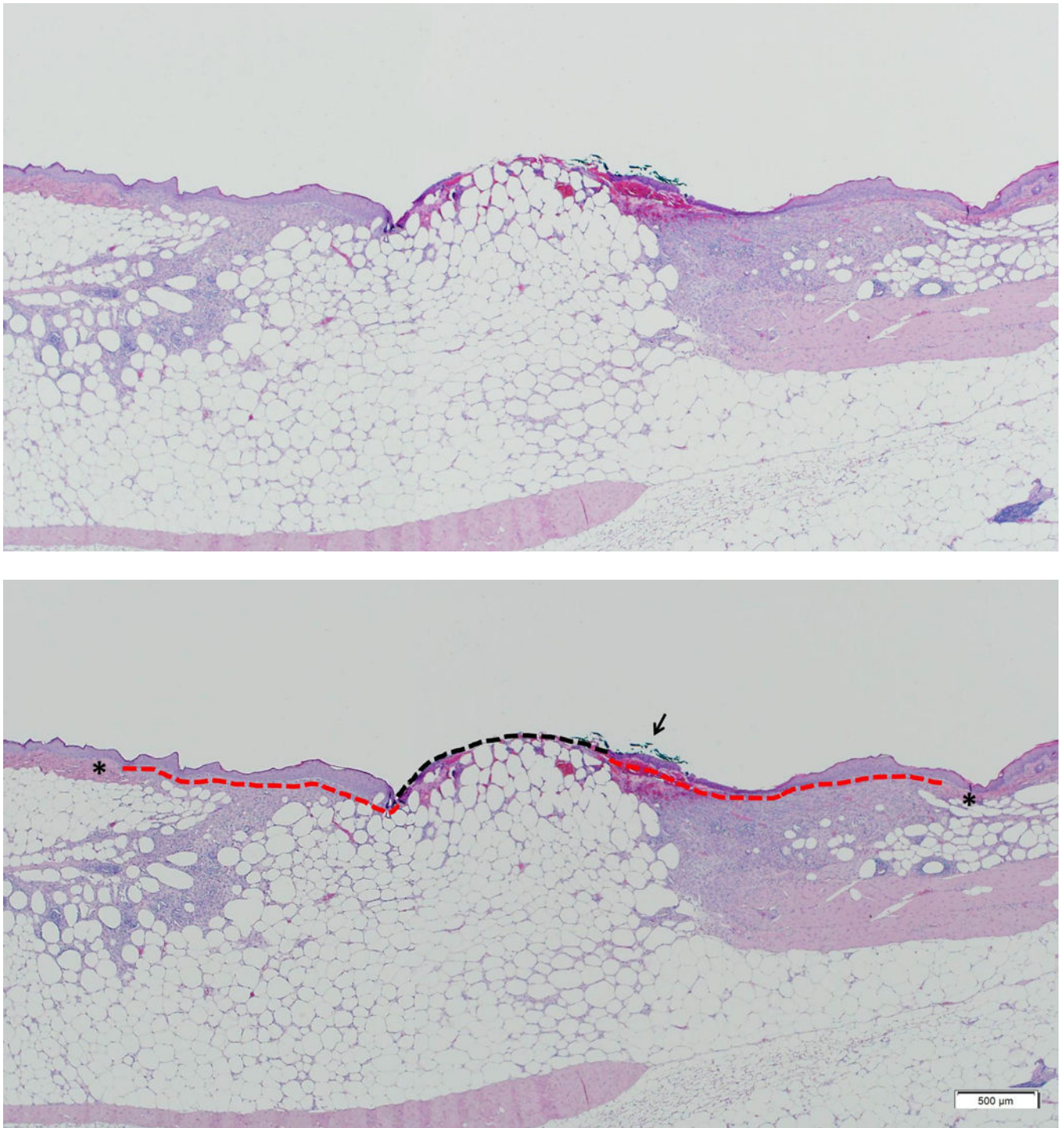
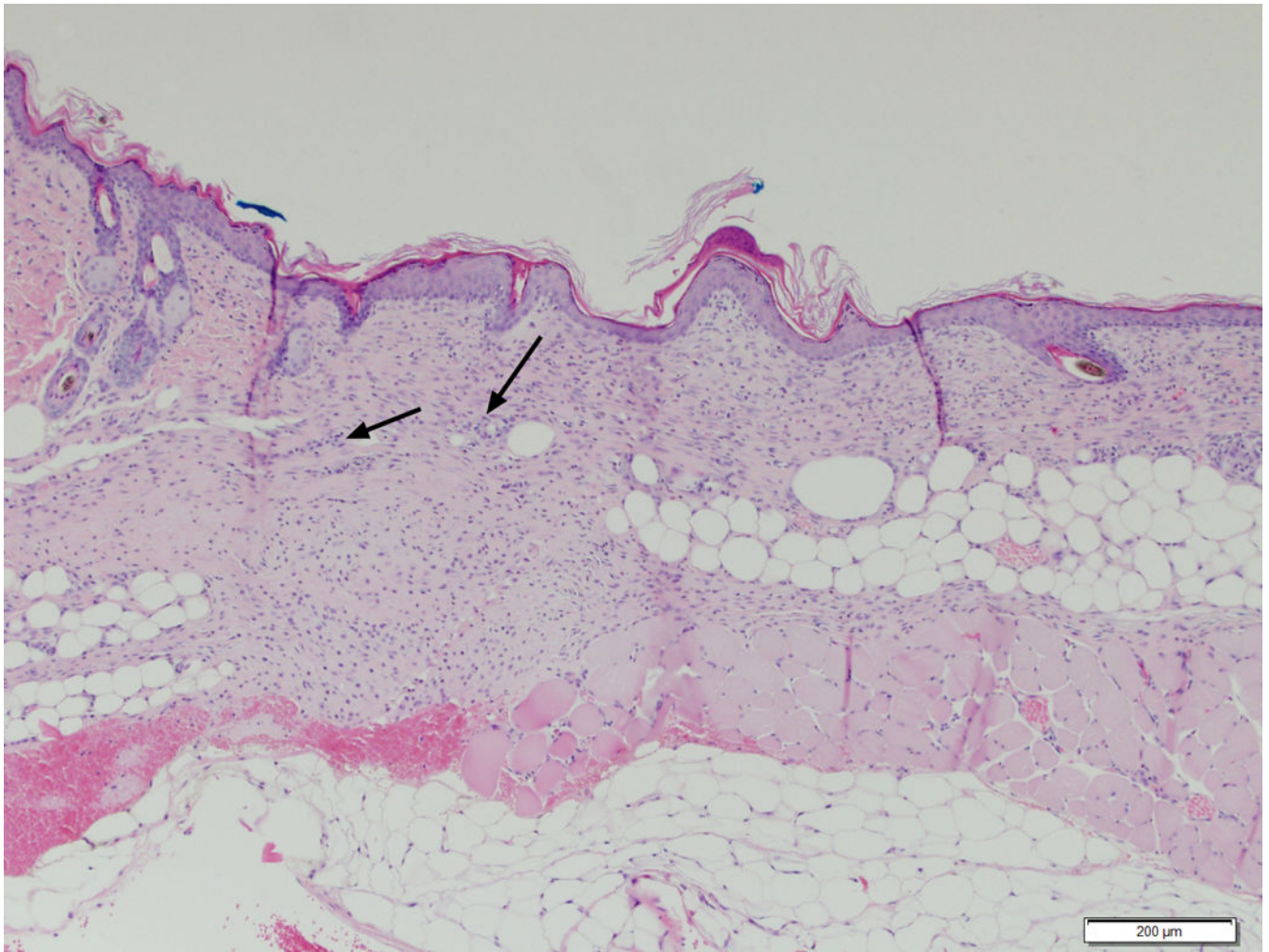


Figure 1. (A) Diabetic mouse wound day 9 post-operatively. (B) Measurement of epithelial gap (dotted black line) and re-epithelialization (red lines). Asterisks identify the native, unaffected dermal tissue. The arrow indicates the green ink used to mark the center of the lesion. Diabetic mouse skin H&E. 20× magnification

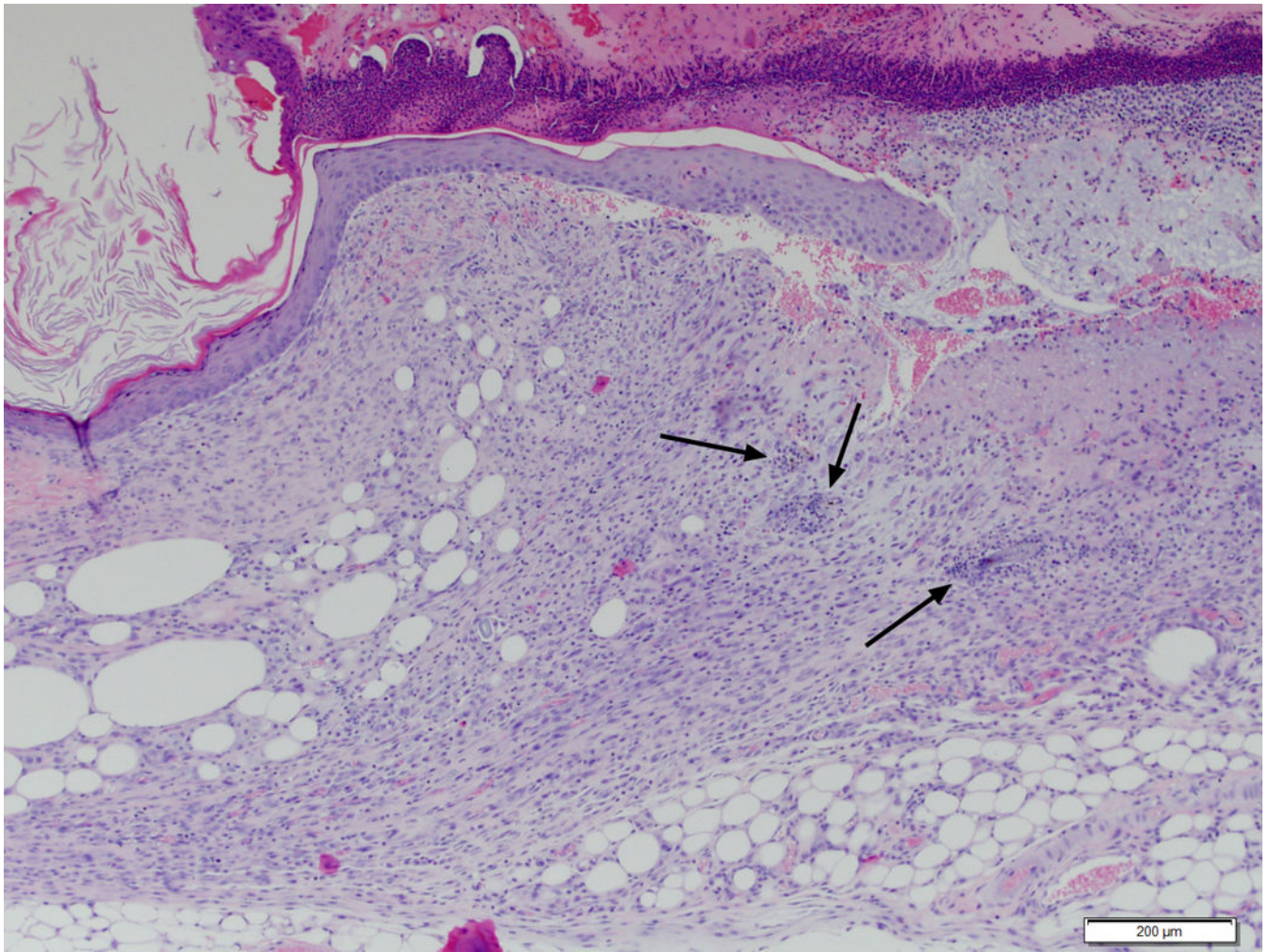


Author Manuscript

Author Manuscript

Author Manuscript

Author Manuscript



Author Manuscript

Author Manuscript

Author Manuscript

Author Manuscript

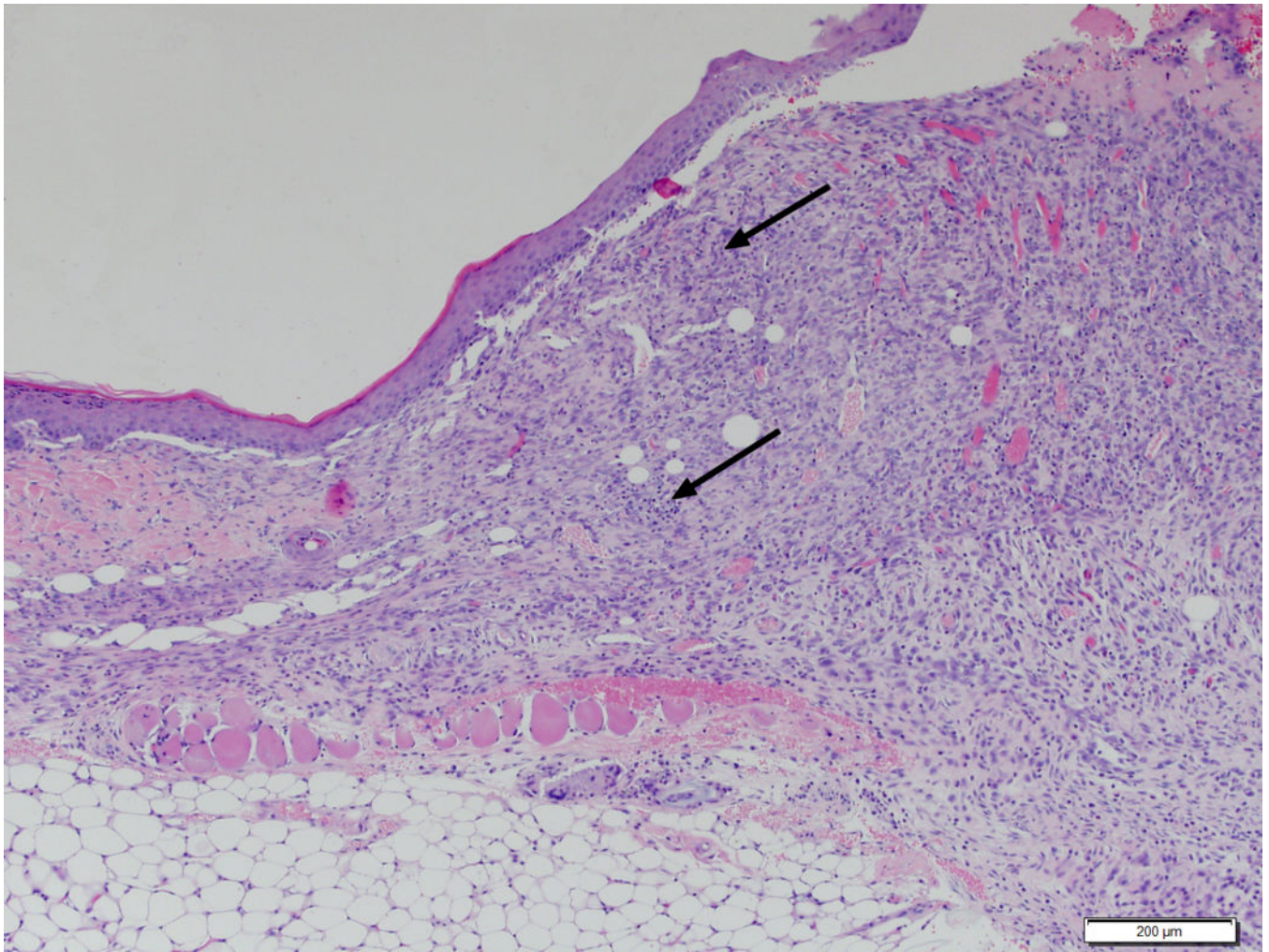
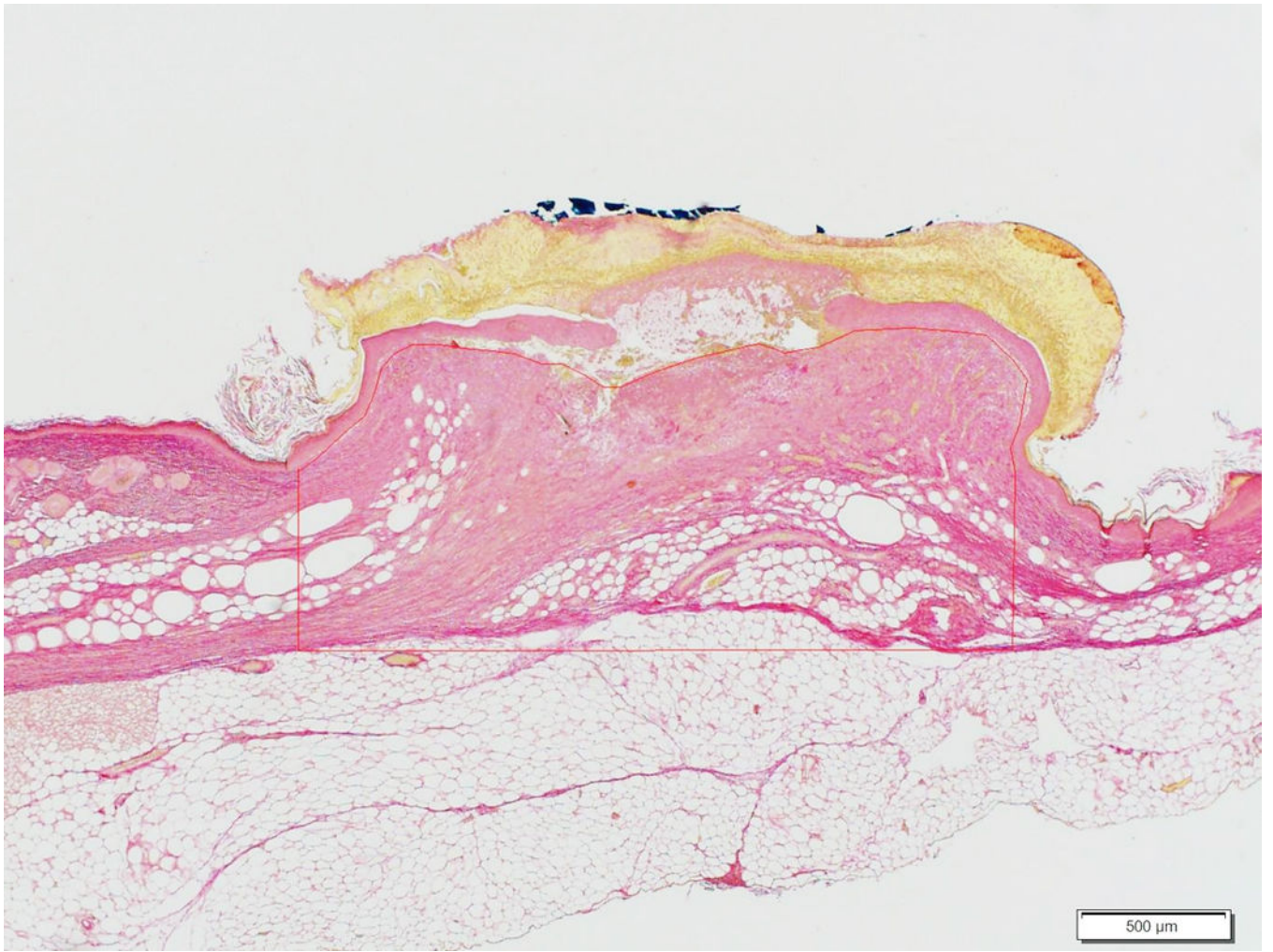


Figure 2. Inflammatory infiltrate in the wound bed. (A) Wound with inflammation score of 1. (B) Wound with inflammation score of 2. (C) Wound with inflammation score of 3. Arrows denote areas of increased inflammatory infiltrate. Diabetic mouse skin H&E. 20× magnification

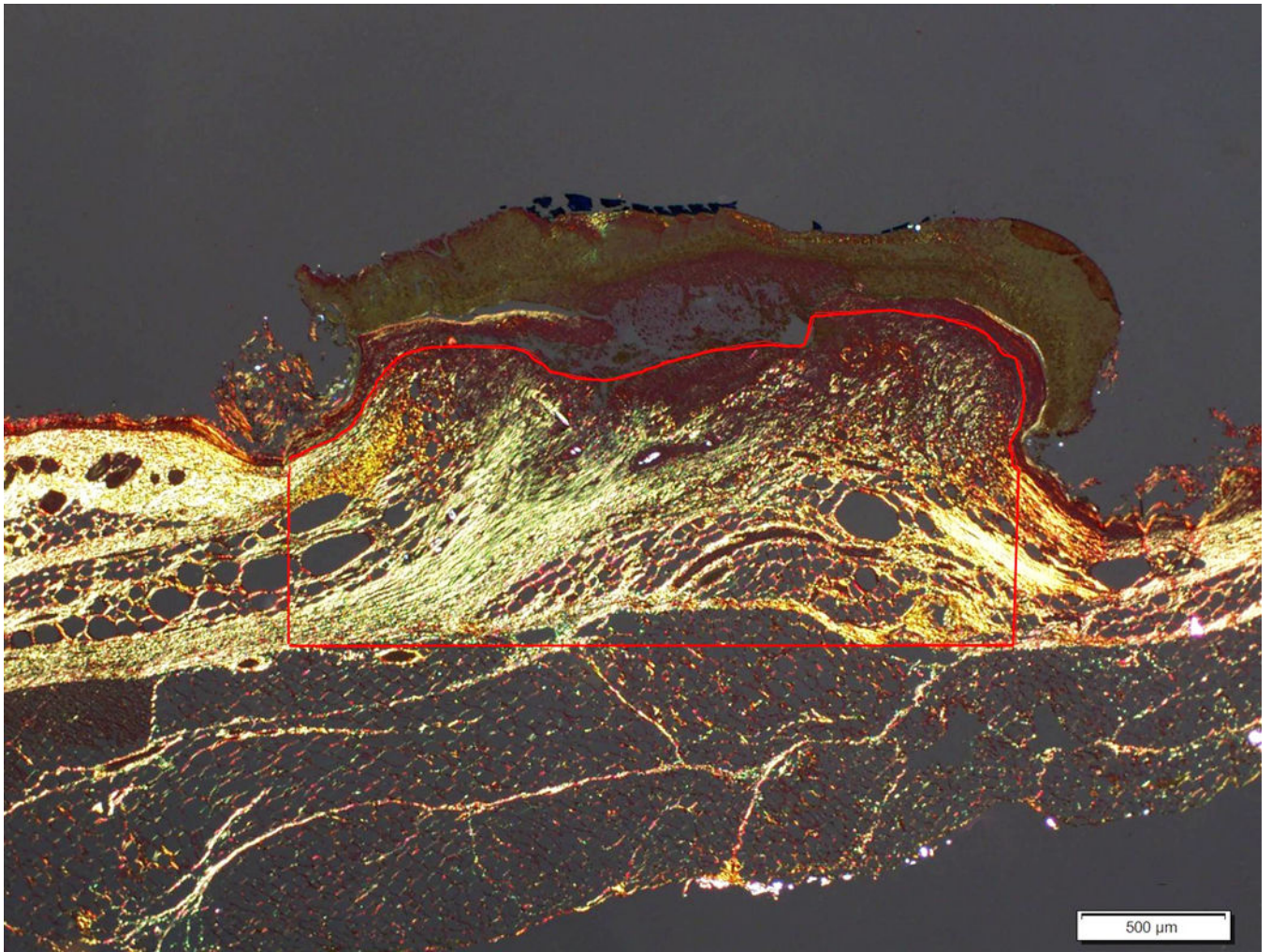


Author Manuscript

Author Manuscript

Author Manuscript

Author Manuscript



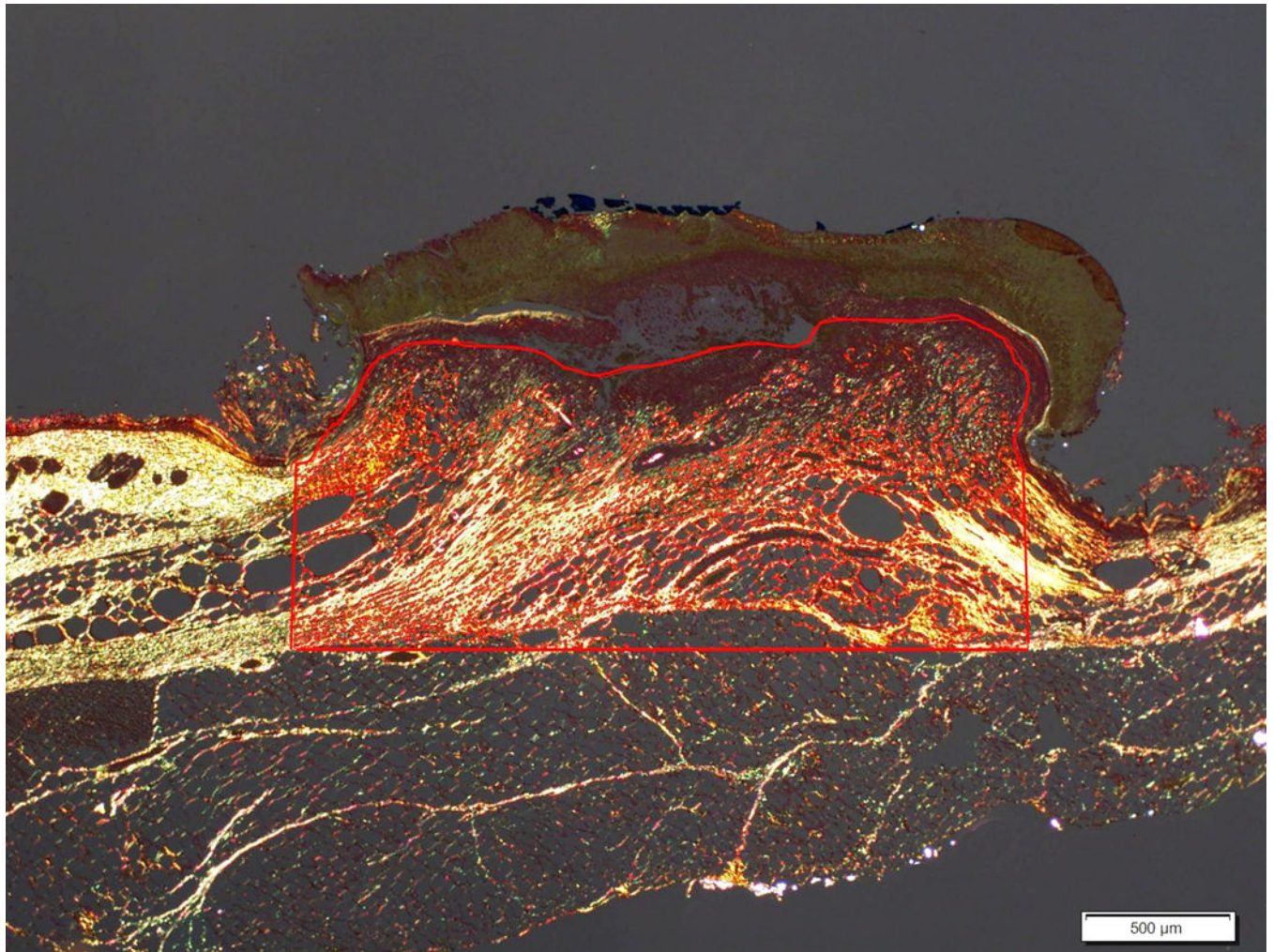
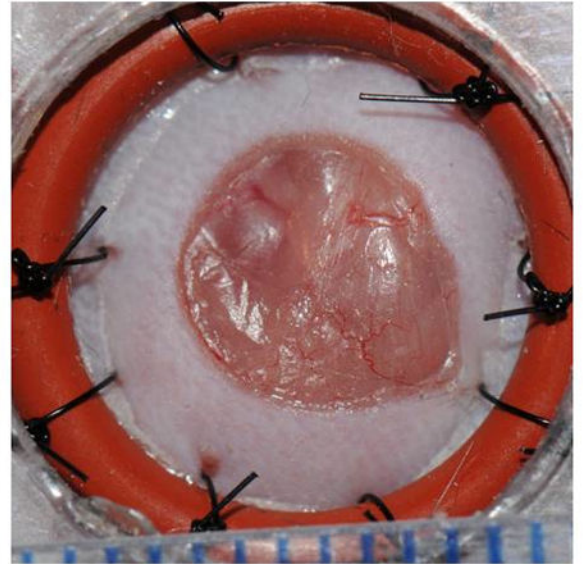
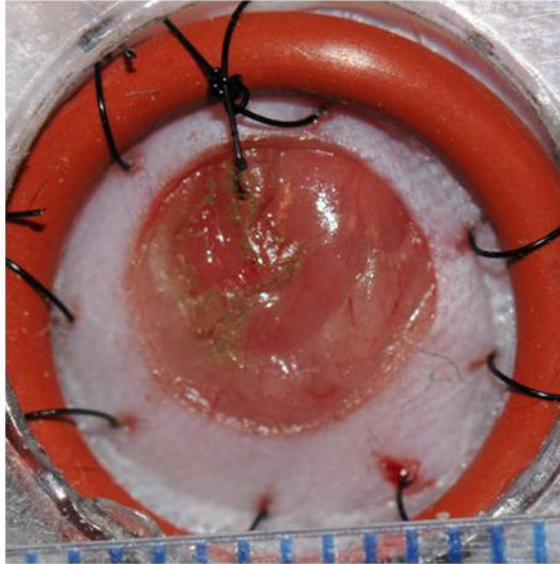
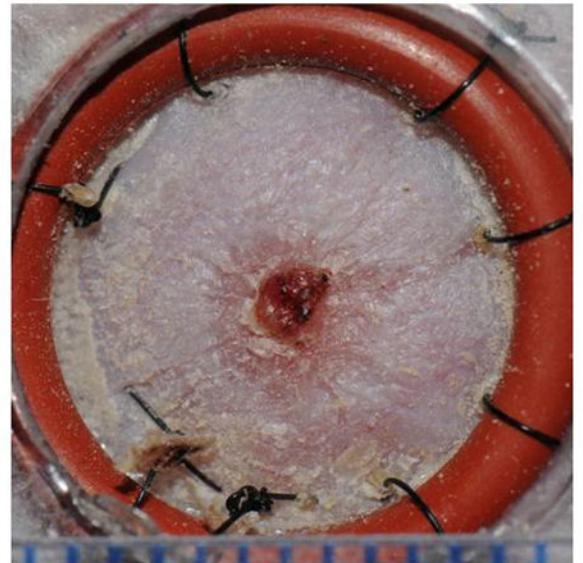
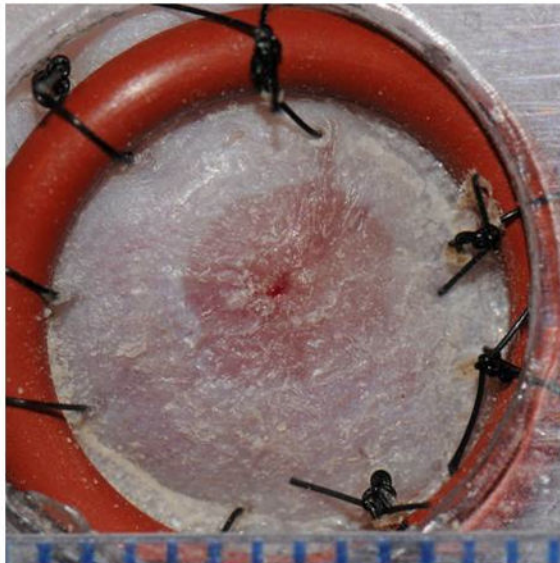


Figure 3. Measurement of the fibrovascular dermal proliferation in the wound bed. (A) The wound bed area in the digital image was outlined (illustrated as red lines) and it comprises a preset depth of 0.75 mm (this is the average depth of the wounds in the experiment) and the borders between preexisting dermal collagen and newly formed collagen. (B) Under polarized light the bright collagen fibers of the wound bed are highlighted. (C) When the wound is stained, software measures the collagen content (only collagen stains) and the final data is expressed as a percentage of outlined wound area. Diabetic mouse skin, Picrosirius red stain. 20× magnification

Silver NP/PEMs**Control****Day 0****Day 9****Figure 4.**

Examples of heterozygous mouse wounds from each experimental group. Top photos are the wounds immediately post-operative. The bottom row shows the same wounds on day 9. Healing was comparable in heterozygous wounds between groups.

Wound closure in heterozygous mice

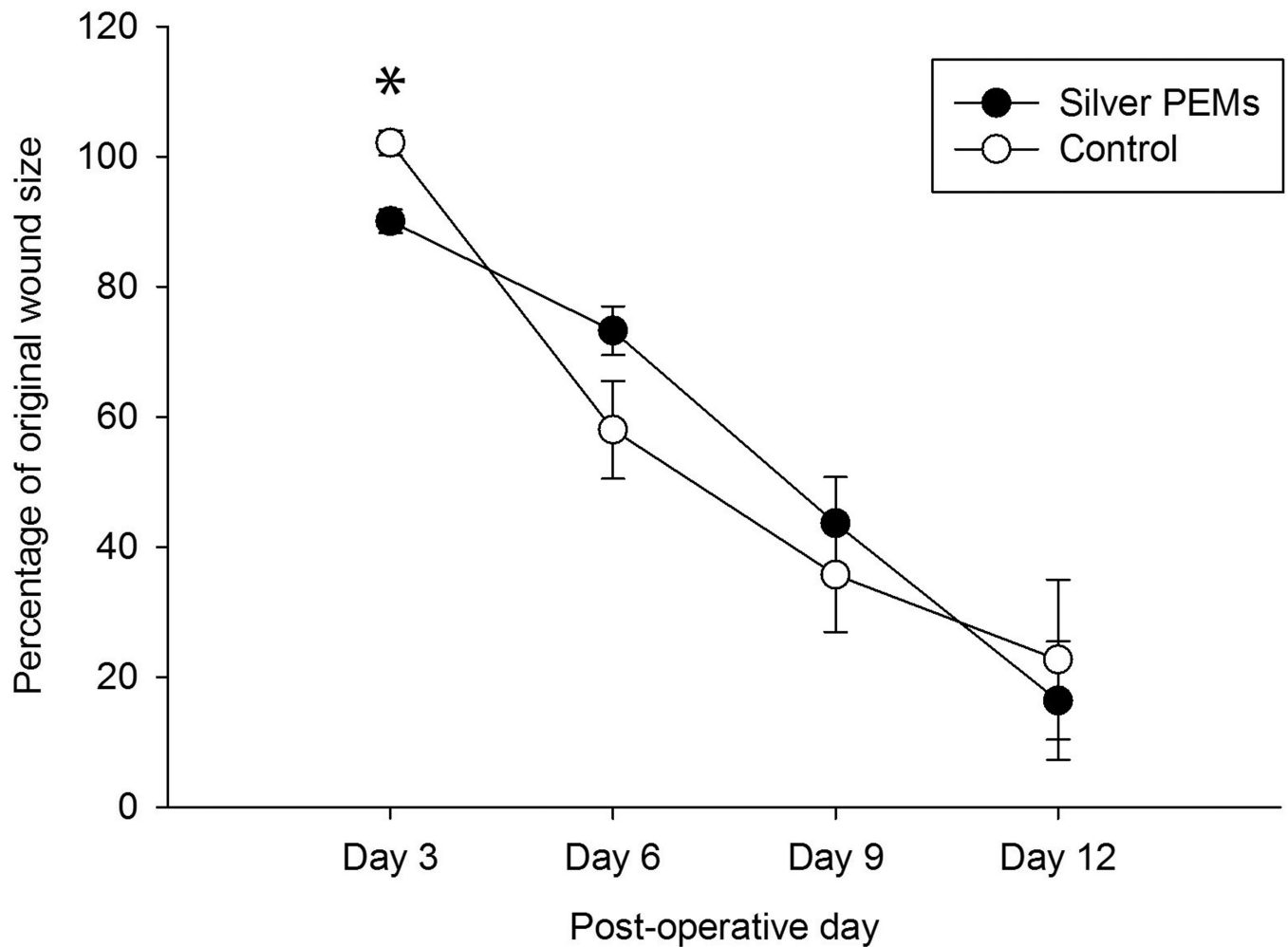


Figure 5.

Mean percentage wound closure in heterozygous mouse wounds with or without silver NP/PEM treatment. Silver-treated wounds were significantly more closed on day 3 versus control group ($p < 0.001$), $n = 10$ mice per group on days 3, 6, and 9 (20 wounds per group; on day 9 there were 9 control wounds and 10 silver-treated wounds). $N = 5$ mice per group on day 12 (7 control wounds and 9 silver-treated wounds). Error bars denote standard error of the mean.

Wound closure in diabetic mice

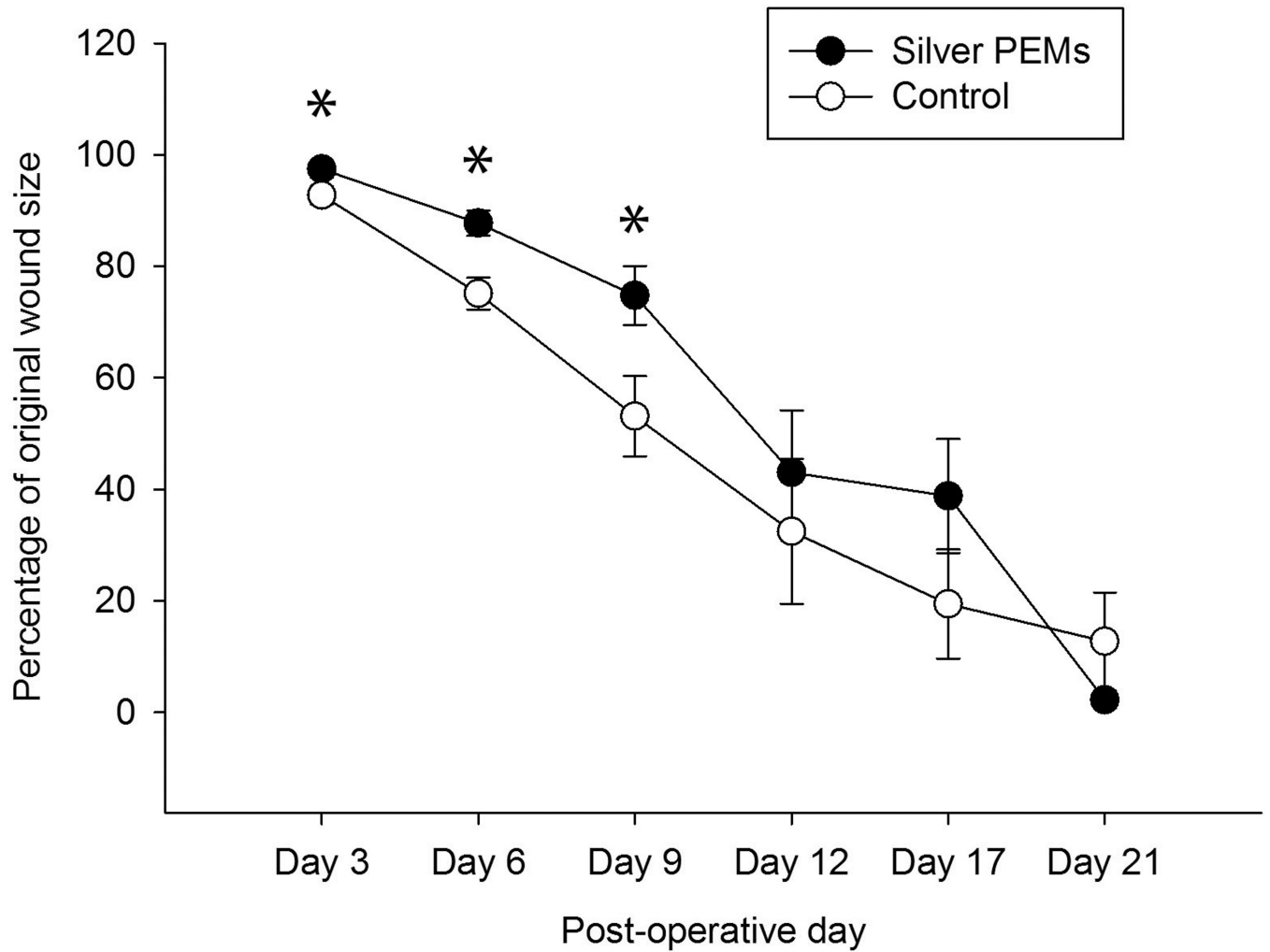


Figure 6.

Mean percentage wound closure in diabetic mouse wounds with or without silver NP/PEM treatment. Wound closure of silver-treated wounds was significantly less on days 3 ($p = 0.041$), 6 ($p = 0.001$), and 9 ($p = 0.017$) but similar thereafter, $n = 10$ mice per group (20 wounds per group) on days 3, 6, and 9. $N = 5$ mice per group on day 12 (10 control wounds, 9 silver-treated wounds), and 5 control and 3 silver-treated mice on days 17 and 21 (10 control wounds and 5 silver-treated wounds). Error bars denote standard error of the mean.

Table 1

Histological analysis of heterozygous mouse wounds on day 9 post-operatively (n = 5 mice per group), and once complete wound closure was noted bilaterally (n = 5 mice per group). On day 9, there was a significantly higher percentage of collagen present (represented by bolded text) in the silver-treated wounds (p = 0.011). Wound size, re-epithelialization, and inflammation scores were not significantly different between groups. At the end of the study, all wounds appeared histologically similar.

	Day 9		End of Study	
	Silver	Untreated	Silver	Untreated
Epithelial gap (diameter mm)	0.45 +/- 0.27	0.45 +/- 0.28	0	0
Re-epithelialization (mm)	4.02 +/- 0.30	3.78 +/- 0.16	3.01 +/- 0.29	2.87 +/- 0.29
Collagen (%)	44.44 +/- 2.17	35.49 +/- 2.13	63.23 +/- 4.55	67.69 +/- 4.65
Inflammation score (0-4)	2.00 +/- 0.21	1.40 +/- 0.18	1.56 +/- 0.24	1.13 +/- 0.29

Table 2

Histological analysis of diabetic mouse wounds on day 9 post-operatively (n = 5 mice per group), and once complete wound closure was noted bilaterally (n = 5 control and 3 silver mice). On day 9, all parameters were significantly different between both groups. Silver-treated wounds were larger ($p < 0.001$), exhibited less re-epithelialization ($p = 0.008$), contained a lower percentage of collagen ($p = 0.011$), and had a higher inflammation score ($p = 0.011$). However, at wound closure, histopathological scores were similar.

	Day 9		End of Study	
	Silver	Untreated	Silver	Untreated
Epithelial gap (diameter mm)	3.93 +/- 0.75	0.40 +/- 0.24	0	0.46 +/- 0.37
Re-epithelialization (mm)	3.76 +/- 0.41	5.41 +/- 0.38	4.82 +/- 0.59	4.07 +/- 0.62
Collagen (%)	20.27 +/- 2.55	29.02 +/- 1.77	35.95 +/- 9.56	23.87 +/- 3.09
Inflammation score (0-4)	2.50 +/- 0.17	1.90 +/- 0.10	2.40 +/- 0.40	2.00 +/- 0.21